Aeroacoustic Optimization Capabilities in the Open-Source SU2 Solver

Beckett Y. Zhou[1,2], Tim Albring[1], Nicolas R. Gauger[1],

Carlos R. Ilario da Silva[3], Thomas D. Economon[3], Juan J. Alonso[3]

[1]Chair for Scientific Computing, TU Kaiserslautern, Germany

[2]Aachen Institute for Advanced Study in Computational Engineering Science (AICES), RWTH Aachen University, Germany

[3]Aerospace Design Laboratory, Stanford University, USA

SU2
The Open-Source CFD Code

March 13, 2018

Challenges in Airframe Noise Reduction – An Optimal Design Perspective

Source: FAA Database

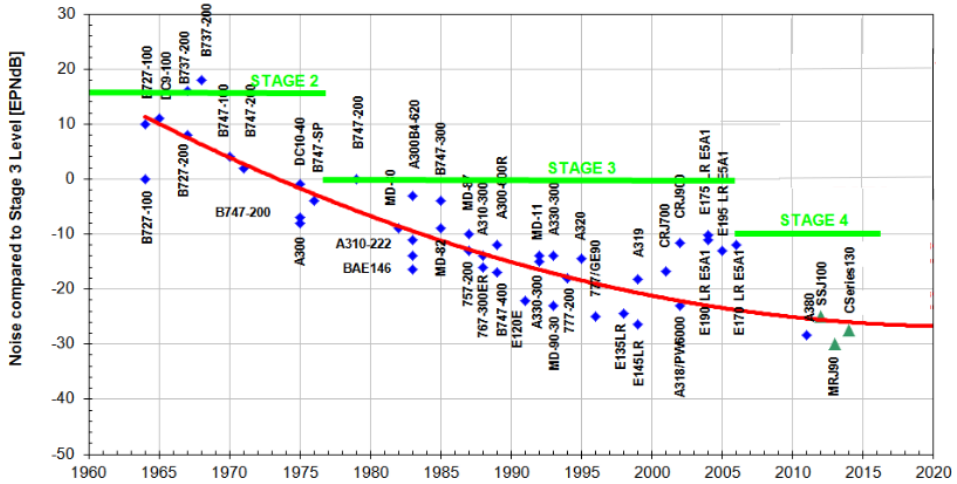

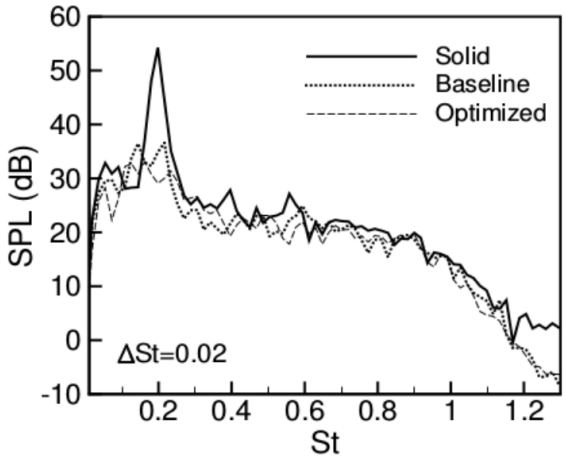

- Various noise sources present at different frequencies but comparable amplitudes – must be reduced by similar amounts for discernible *overall* noise reduction
- $J^N = rms(p')$(=OASPL) misleading
  - Must target broadband component!
  - EPNLdB (2-10kHz range)
  - Strong requirement on CAA solver
- To meet aggressive noise reduction goals, it is insufficient to only reduce high-lift and landing gear noise – trailing edge scattering ('lower bound') must be reduced.(1)
- Require efficient simulation and design tools to explore innovative and unconventional configurations and control strategies
  - Porous TE
  - LE and TE serrations
  - ...

(1). D. P. Lockard and G. M. Lilley, *The Airframe Noise Reduction Challege*, NASA Report 2004-213013

Review of Existing Work

State of the Art on Aeroacoustic Simulation

- 'Direct' noise computation via DNS/LES computationally intractable for far-field observer locations (strong disparity between hydrodynamic and acoustic length scales at low M_∞)
- A hybrid two-stage approach allows for more efficient noise prediction
- Near-body turbulent flow field resolved using LES/DES/URANS
- Noise signal propagated to far-field using linearized Euler or integral methods such as Ffowcs Williams-Hawkings (FW-H)
- **Predicitive capabilities must be used to influence design!**

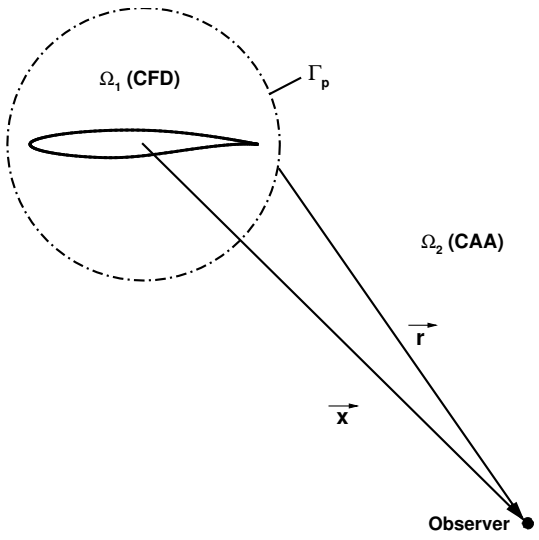

Computational Cost: $(N_{xyz} \sim 10^8) \times (N_{\Delta t} \sim 10^5) \implies$ CPU-hrs $\sim$?

Existing Work on Aeroacoustic Optimization – A Non-Exhaustive List

- Airfoil design in turbulent flow (2D URANS+FW-H) using discrete adjoint, Rumpfkeil & Zingg, 2010
- Helicopter blade design (3D Euler+FW-H) using discrete adjoint, Fabiano et al., 2015
- Optimal control of shear-layer noise (DNS) using continuous adjoint, Buchta et al. 2016
- Porous trailing-edge design (LES+APE) using AD-based discrete adjoint, Zhou, Gauger et al., 2015, 2016
- **Optimizations involving high-fidelity and scale-resolving simulations limited to simple geometries**

Review of Existing Work

State of the Art on Aeroacoustic Simulation

- 'Direct' noise computation via DNS/LES computationally intractable for far-field observer locations (strong disparity between hydrodynamic and acoustic length scales at low M_∞)
- A hybrid two-stage approach allows for more efficient noise prediction
- Near-body turbulent flow field resolved using LES/DES/URANS
- Noise signal propagated to far-field using linearized Euler or integral methods such as Ffowcs Williams-Hawkings (FW-H)
- **Predicitive capabilities must be used to influence design!**

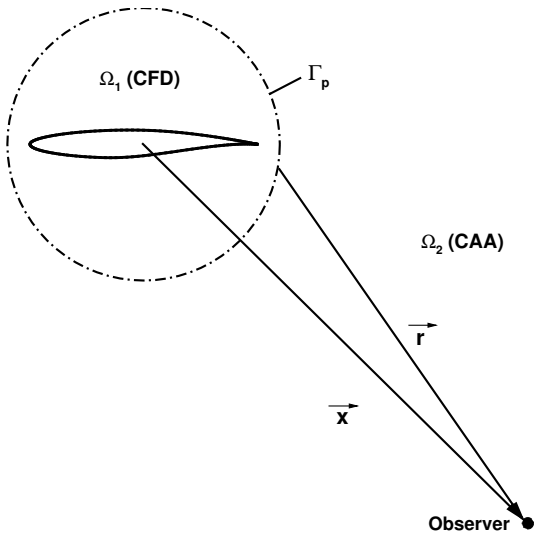

Computational Cost: $(N_{xyz} \sim 10^8) \times (N_{\Delta t} \sim 10^5) \implies$ CPU-hrs $\sim$?

Existing Work on Aeroacoustic Optimization – A Non-Exhaustive List

- Airfoil design in turbulent flow (2D URANS+FW-H) using discrete adjoint, Rumpfkeil & Zingg, 2010
- Helicopter blade design (3D Euler+FW-H) using discrete adjoint, Fabiano et al., 2015
- Optimal control of shear-layer noise (DNS) using continuous adjoint, Buchta et al. 2016
- Porous trailing-edge design (LES+APE) using AD-based discrete adjoint, Zhou, Gauger et al., 2015, 2016
- **Optimizations involving high-fidelity and scale-resolving simulations limited to simple geometries**

This work: Consistent and robust discrete adjoint on the basis of algorithmic differentiation (AD) to explore unconventional design concepts

SU2 – An Open-Source Multi-Physics Analysis and Design Tool

SU2
The Open-Source CFD Code

- Open source multi-physics solver suite
- URANS: FV method with various flux discretization schemes (JST, AUSM, etc) and turbulence models (SA & SST) implemented
- Dual-time stepping for time-accuracy
- Dynamic grid movement capability
- SLSQP optimizer (SciPy), initially implemented with continuous adjoint

Active development on various disciplines by many groups around the world

- Stanford University (original solver, continueous adjoint, etc)
- TU Kaiserslautern (CFD-CAA coupled solver, AD-based discrete adjoint)
- TU Delft & Politecnico di Milano (Turbomachinery applications)
- Imperial College (Aero-structural analysis)
- Technological Institute of Aeronautics (DDES, IDDES, etc)

Latest Version (v6.0 Falcon) released in Feb. 2018

Aeroacoustic Simulation and Optimization in SU2 – The Past, Present, and Future

Past

- 2D URANS+FWH in frequency domain
- Noise minimization on various 2D configurations

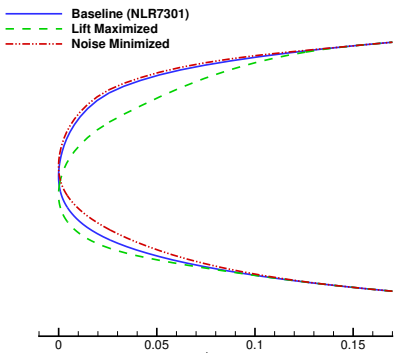

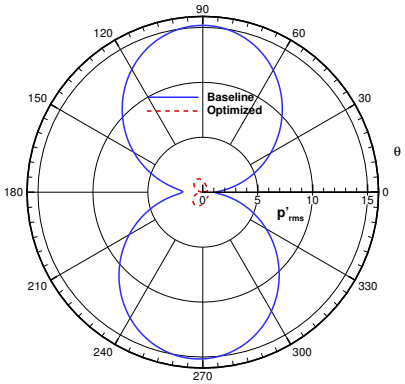

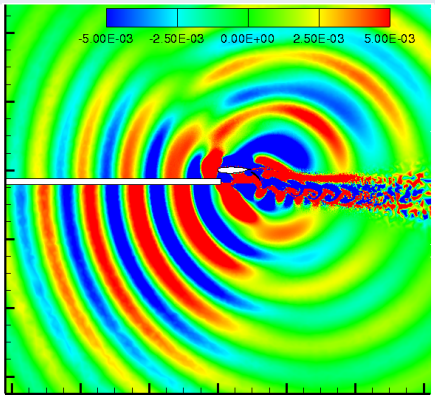

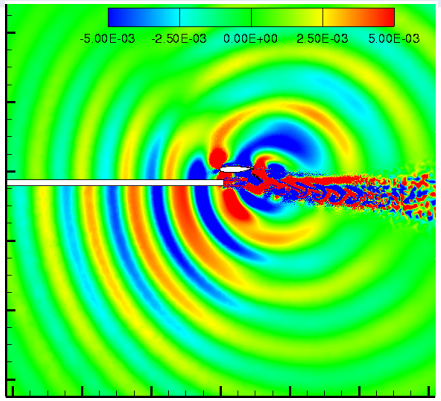

AVIATION 2016

SCI-TECH 2017

Aeroacoustic Simulation and Optimization in SU2 – The Past, Present, and Future

Past

- 2D URANS+FWH in frequency domain
- Noise minimization on various 2D configurations

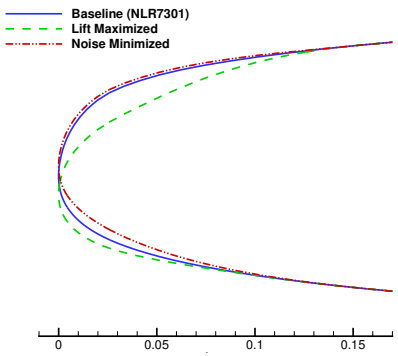

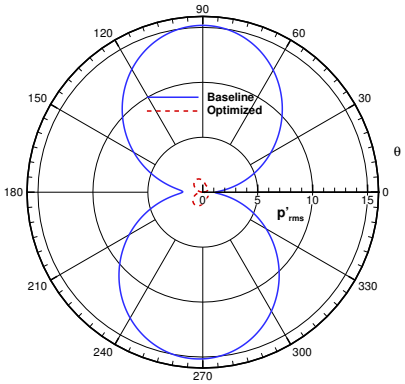

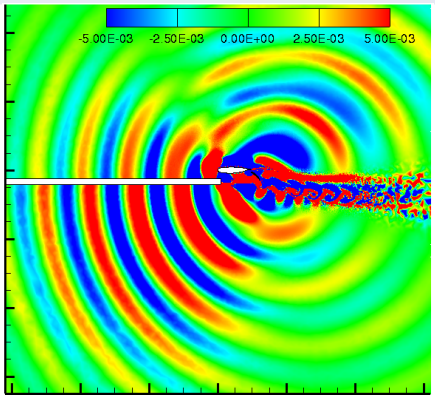

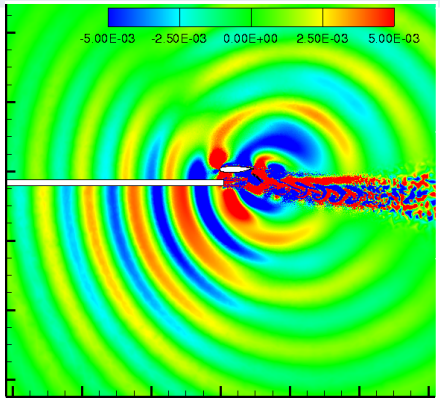

Present

- 3D FWH in both time and frequency domain, coupled with URANS and DDES
- Noise minimization with 3D URANS+FWH, final analysis using DDES+FWH
- Preliminary validation against experiment using DDES+FWH

Future

- Minimization of broadband noise with DDES+FWH
- (U)RANS with stochastic noise generation (SNGR/fRPM/ASR)

A Coupled CFD-CAA Framework for Noise Prediction

A boundary integral formulation of the permeable surface **F**fowcs **W**illiams-**H**awkings (FW-H) acoustic solver is coupled with CFD solver in SU2 for efficient acoustic computations at arbitrary observer locations. [Di Francescantonio, 1997]

$$p'_{obs}(\vec{x},t) = \underbrace{\int_{\Gamma_p}\left[\frac{\rho_\infty \dot{U}\cdot\hat{n}}{4\pi r}\right]_{ret} d\Gamma_p}_{p'_T} + \underbrace{\frac{1}{c}\int_{\Gamma_p}\left[\frac{\dot{F}\cdot\hat{r}}{4\pi r}\right]_{ret} d\Gamma_p + \int_{\Gamma_p}\left[\frac{F\cdot\hat{r}}{4\pi r^2}\right]_{ret} d\Gamma_p}_{p'_L} + p'_Q \qquad (1)$$

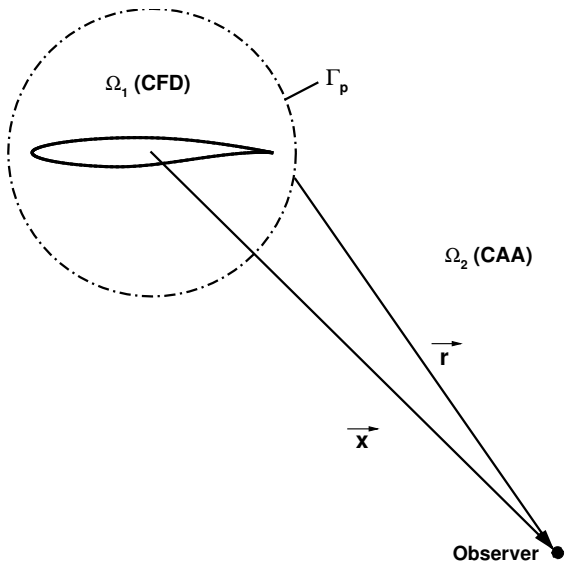

where

$$U_i = \rho u'_i/\rho_\infty,$$

$$F_i = \left[(p-p_\infty)\delta_{ij} - \tau_{ij} + \rho u'_i u'_j\right]\hat{n}_j,$$

- Flow field in Ω_1 resolved by CFD
- p, ρ, u'_i on Γ_p extracted from CFD data
- p'_T & p'_L: 'thickness' and 'loading' noise source
- Quadrupole source (p'_Q) negligible for low M_∞
- $[\cdot]_{ret}$: source terms evaluated in 'retarded' time
- 2-D freq-domain formulation also implemented (Lockard, 2000)

AD-based Unsteady Discrete Adjoint Framework

Consider a system of semi-discretized PDEs as follows:

$$\frac{dU}{dt} + R(U) = 0$$

U: spatially discretized state vector
$R(U)$: is the discrete spatial residual vector.

Second-order backward difference is used for time discretization:

$$R^*(U^n) = \frac{3}{2\Delta t}U^n + R(U^n) - \frac{2}{\Delta t}U^{n-1} + \frac{1}{2\Delta t}U^{n-2} = 0, \quad n = 1, \ldots, N$$

Dual-time stepping method converges $R^*(U^n)$ to a steady state solution at each time level n through a pseudo time τ:

$$\frac{dU^n}{d\tau} + R^*(U^n) = 0$$

Implicit Euler method is used to time march the above equation to steady state:

$$U^n_{p+1} - U^n_p + \Delta\tau R^*(U^n_{p+1}) = 0, \qquad p = 1, \ldots, M$$

AD-based Unsteady Discrete Adjoint Framework

The resultant nonlinear system can be linearized around U_p^n to solve for the state U_{p+1}^n:

$$U_{p+1}^n - U_p^n + \Delta\tau \left[R^*(U_p^n) + \left.\frac{\partial R^*}{\partial U}\right|_p^n (U_{p+1}^n - U_p^n) \right] = 0, \qquad p = 1, \ldots, M$$

This can be written in the form of a fixed-point iteration:

$$U_{p+1}^n = G^n(U_p^n, U^{n-1}, U^{n-2}), \qquad p = 1, \ldots, M, \qquad n = 1, \ldots, N$$

G^n: an iteration of the pseudo time stepping
U^{n-1}: converged state vector at time level $n-1$
U^{n-2}: converged state vectors at time level $n-2$

The fixed point iteration converges to the numerical solution U^n:

$$U^n = G^n(U^n, U^{n-1}, U^{n-2}), \qquad n = 1, \ldots, N$$

AD-based Unsteady Discrete Adjoint Framework

The discretized unsteady optimization problem over N time levels:

$$\begin{aligned} \min_{\alpha} \quad & J = f(U^{N_*}, \ldots, U^N, \alpha) \\ \text{subject to} \quad & U^n = G^n(U^n, U^{n-1}, U^{n-2}, \alpha), \qquad n = 1, \ldots, N \end{aligned}$$

α: vector of design variables. J is evaluated between $N_* \leq n \leq N$. One can express the Lagrangian associated with the above constrained optimization problem as follows:

$$L = f(U^{N_*}, \ldots, U^N, \alpha) - \sum_{n=1}^{N} [(\bar{U}^n)^T (U^n - G^n(U^n, U^{n-1}, U^{n-2}, \alpha))]$$

$\bar{U}^n$: adjoint state vector at time level n.

$$KKT: \quad \begin{aligned} \frac{\partial L}{\partial \bar{U}^n} &= 0, \quad n = 1, \ldots, N && \text{(State equations)} \\ \frac{\partial L}{\partial U^n} &= 0, \quad n = 1, \ldots, N && \text{(Adjoint equations)} \\ \frac{\partial L}{\partial \alpha} &= 0, && \text{(Control equation)} \end{aligned}$$

AD-based Unsteady Discrete Adjoint Framework

The unsteady discrete adjoint equations can be derived in the fixed point form as:

$$\bar{U}^n_{i+1} = \underbrace{\left(\frac{\partial G^n}{\partial U^n}\right)^T \bar{U}^n_i + \left(\frac{\partial G^{n+1}}{\partial U^n}\right)^T \bar{U}^{n+1} + \left(\frac{\partial G^{n+2}}{\partial U^n}\right)^T \bar{U}^{n+2}}_{\bar{G}^n(\bar{U}^n, \bar{U}^{n-1}, \bar{U}^{n-2})} + \left(\frac{\partial J}{\partial U^n}\right)^T, \quad n = N, \ldots, 1$$

$\bar{U}^{n+1}$: converged adjoint state vector at time level $n+1$
$\bar{U}^{n+2}$: converged adjoint state vector at time level $n+2$

The unsteady adjoint equations above are solved backward in time.
The sensitivity gradient can be computed from the adjoint solutions:

$$\frac{dL}{d\alpha} = \frac{\partial J}{\partial \alpha} + \sum_{n=1}^{N} \left((\bar{U}^n)^T \frac{\partial G^n}{\partial \alpha} \right)$$

- High-lighted terms computed using Algorithmic Differentiation in reverse mode
- Reverse accumulation used at each time level to 'tape' the computational graph for AD
- Adjoint iterator inherits the same convergence properties as primal iterator
- G includes: turbulence model, grid movement, limiters, etc
- AD implementation details see Albring et al. AIAA-2016-3518

Coupled CFD-FWH Noise Prediction and Optimization Framework

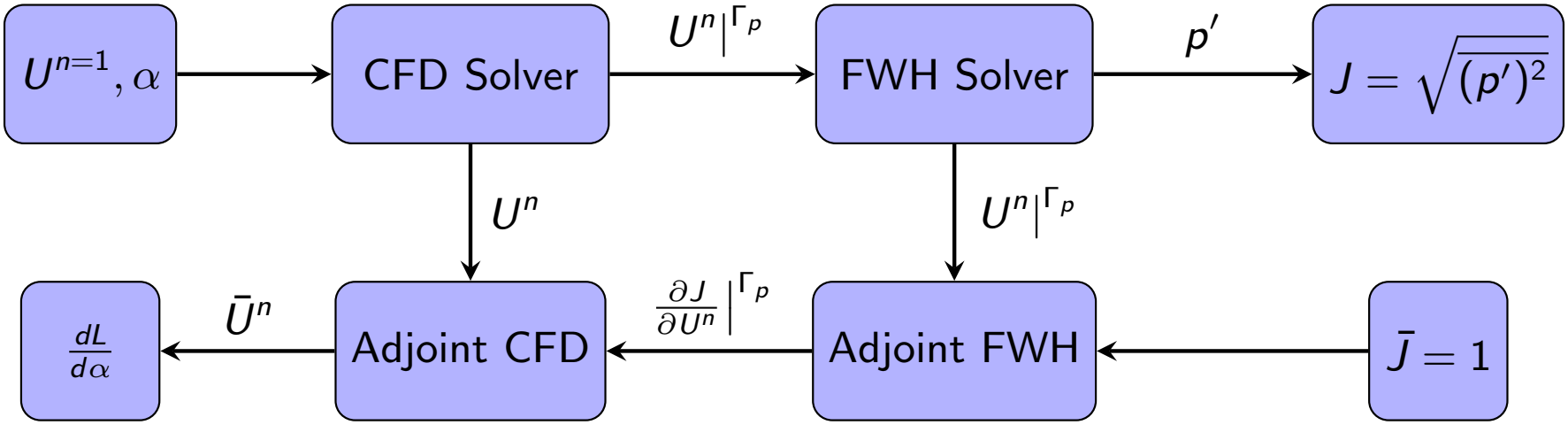

- CFD Solver: $U^n = G^n(U^n, U^{n-1}, U^{n-2})$
- FWH Solver: $p'_{obs}(\vec{x}, t) = p'_T + p'_L = Fn(\, U|^{\Gamma_p}, \vec{x}, t)$
- Adjoint CFD: $\bar{U}^n = \bar{G}^n(\bar{U}^n, \bar{U}^{n-1}, \bar{U}^{n-2}) + (\, \frac{\partial J}{\partial U^n}\Big|^{\Gamma_p})^T$
- $U^n|^{\Gamma_p}$: Flow variables at time step n on the FWH surface Γ_p
- $\frac{\partial J}{\partial U^n}\Big|^{\Gamma_p}$: sensitivity of the noise objective with respect to flow variables evaluated on the FWH surface Γ_p

Verification of FWH Solver (2D)

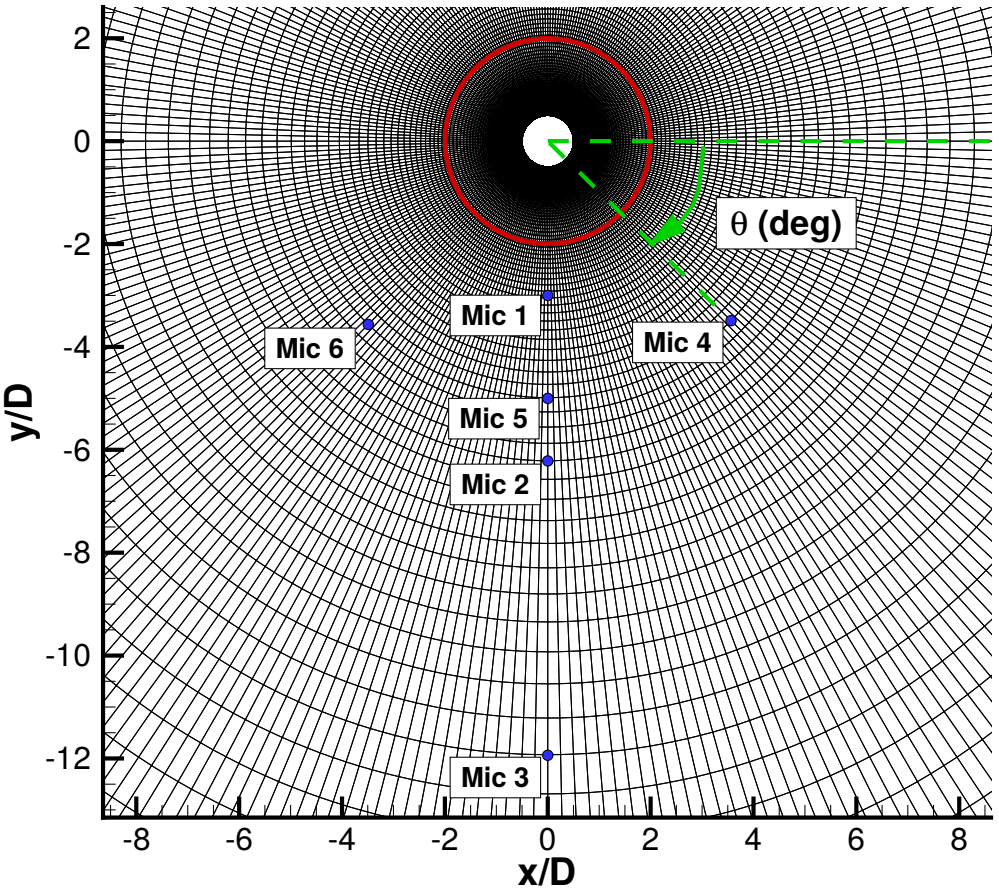

- 2-D circular cylinder in subsonic, turbulent flow
- $M_\infty = 0.25$, $Re = 5 \times 10^6$
- Turbulent flow computed by URANS
- Acoustics computed by 2-D freq-domain FWH (Lockhard, 2000)
- 3 mics placed in radial direction and 3 mics in circumferential direction
- p' at mic positions compared (URANS-FWH vs. Direct URANS)

Microphone No.	r	θ
1	3D	90°
2	6D	90°
3	12D	90°
4	5D	45°
5	5D	90°
6	5D	135°

Verification of 2-D FWH Solver (Circumferential Direction)

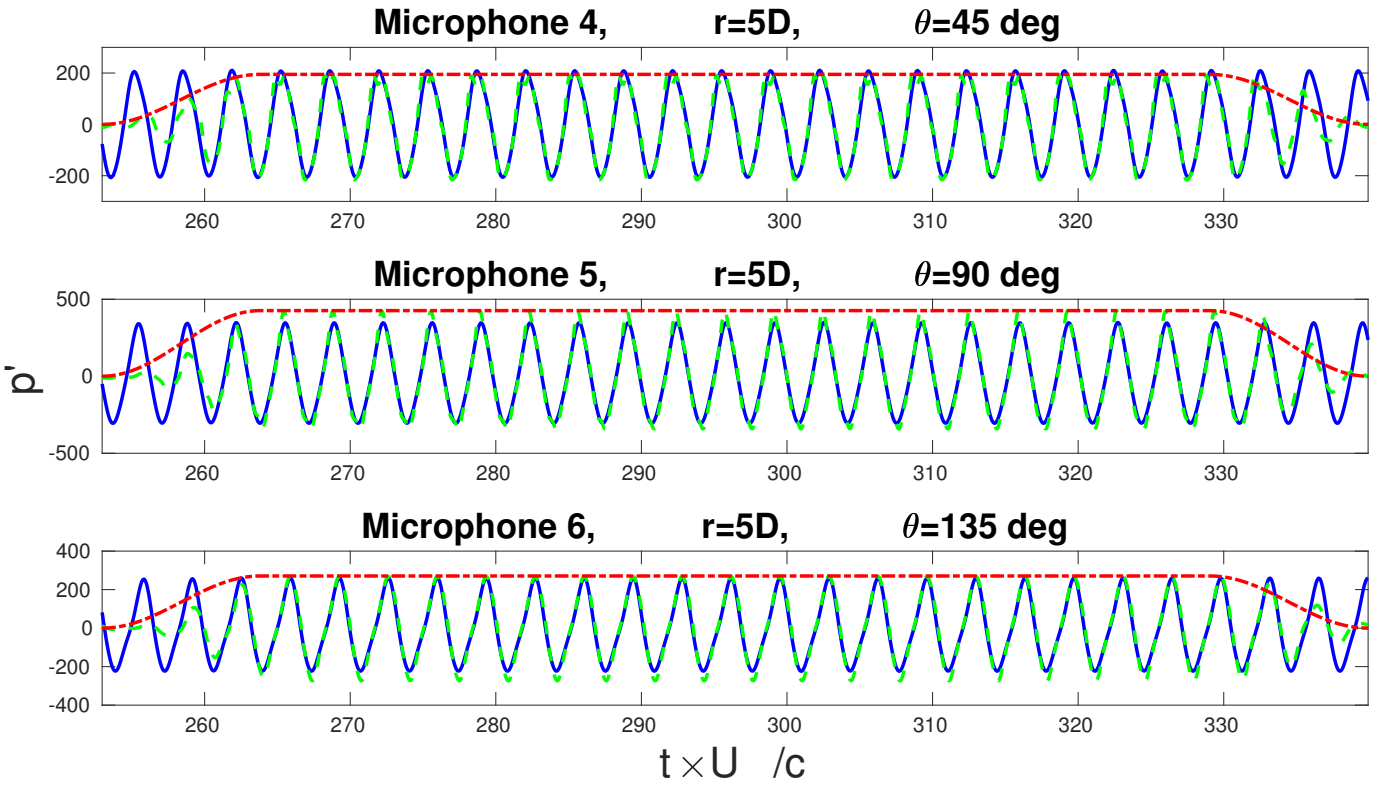

——: Direct URANS; – – – : URANS-FWH; -·-·-: Hanning Window

- Excellent match in frequency
- Slight mismatch in amplitude – Hanning window (to enforce periodicity) is energy-preserving, NOT amplitude-preserving

Verification of 2-D FWH Solver (Radial Direction)

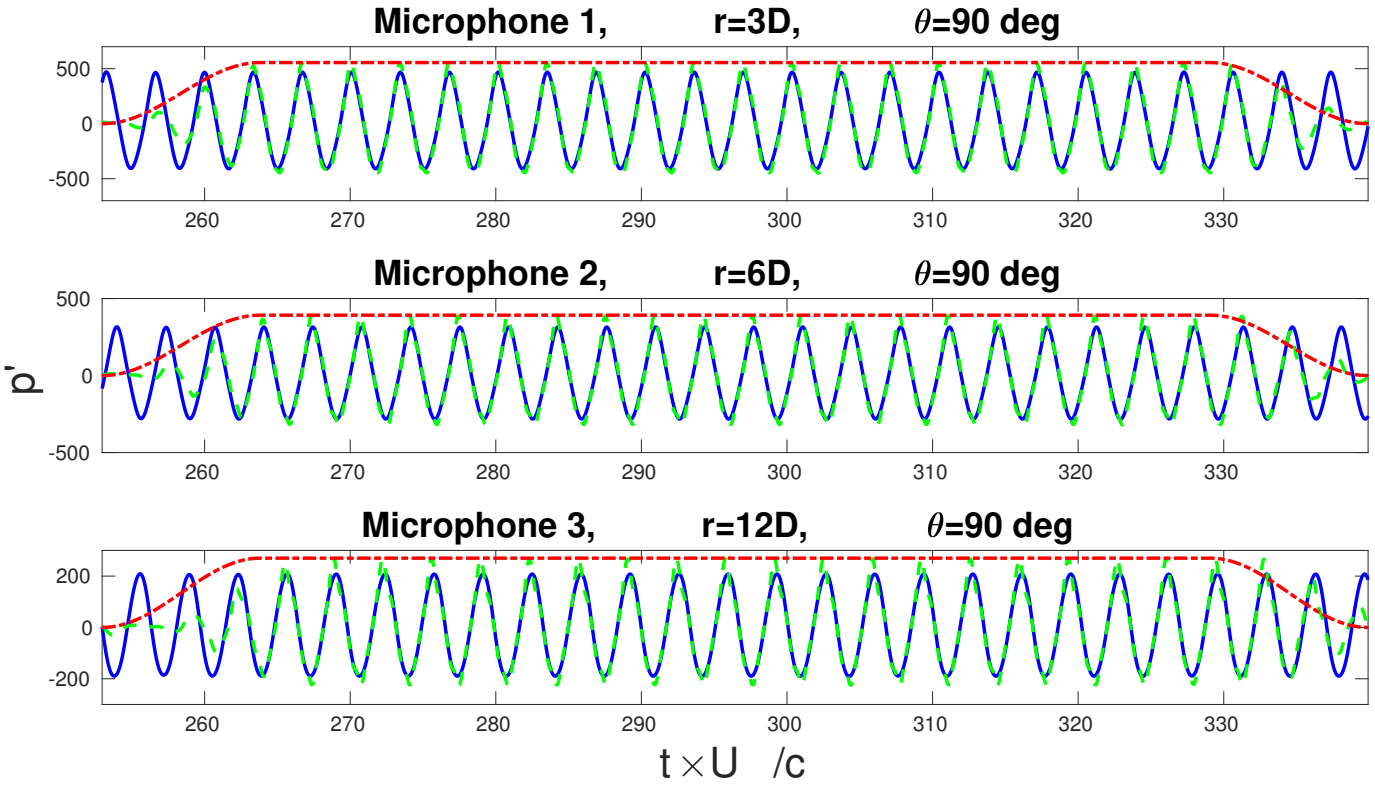

——: Direct URANS; – – – : URANS-FWH; -·-·-: Hanning Window

- Excellent match in frequency
- Discernible amplitude difference in furthest mic (r=12D) due to mesh coarsening (damping of static pressure signal in URANS)

Verification of FWH Solver (3-D)

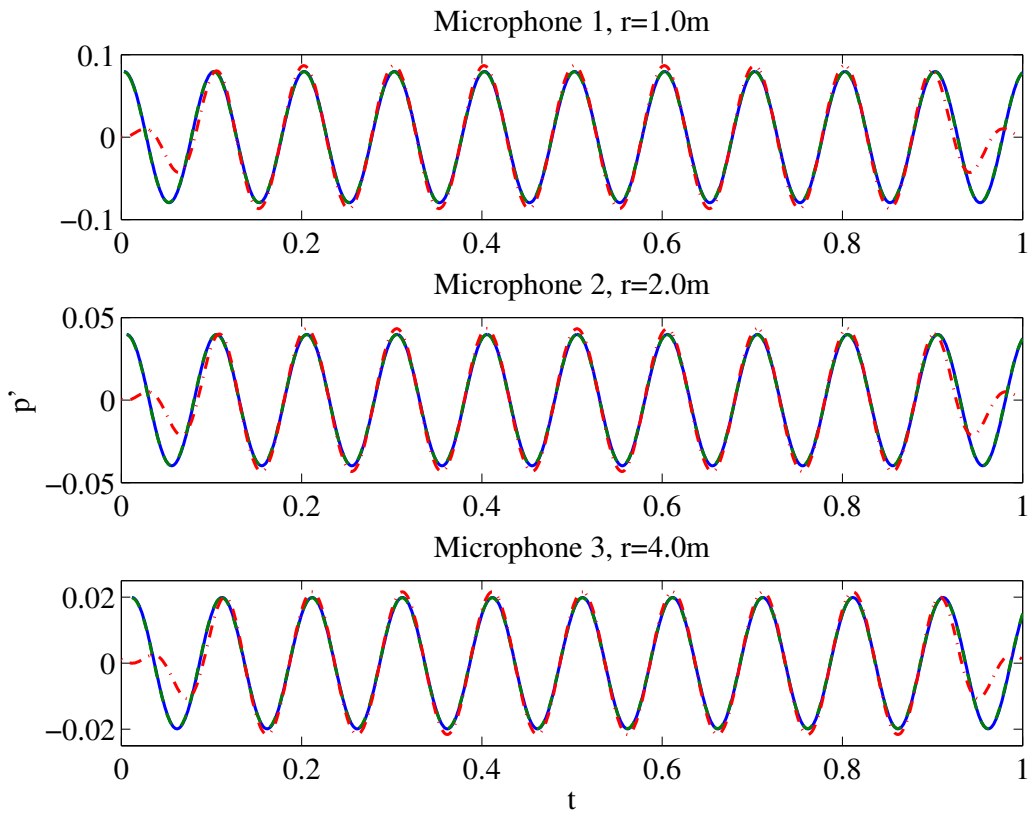

Analytic: (——)
Time-domain FWH: (– – –)
Frequency-domain FWH: (-·-·-)

- Monopole source at origin
- Acoustic source on FWH surface analytically computed
- Propagation to farfield with both time- and frequency-domain FWH
- Excellent agreement between FWH-propagated signal and analytical signal at 3 farfield positions
- Slight mis-match in amplitude for frequency-domain FWH due to windowing
- Farfield $p' \propto 1/r$ scaling law perfectly observed

Validation: 3-D Rod-Airfoil Configuration

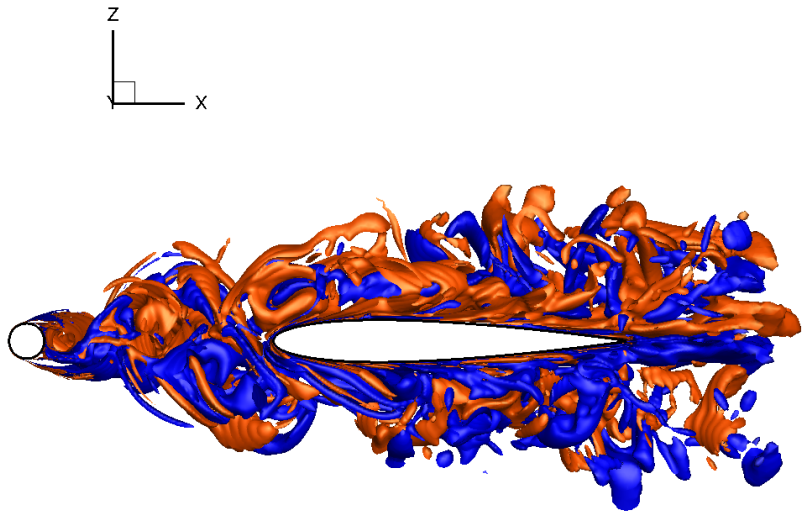

Vorticity Iso-surfaces ($\omega_z D/U_\infty = \pm 1$)

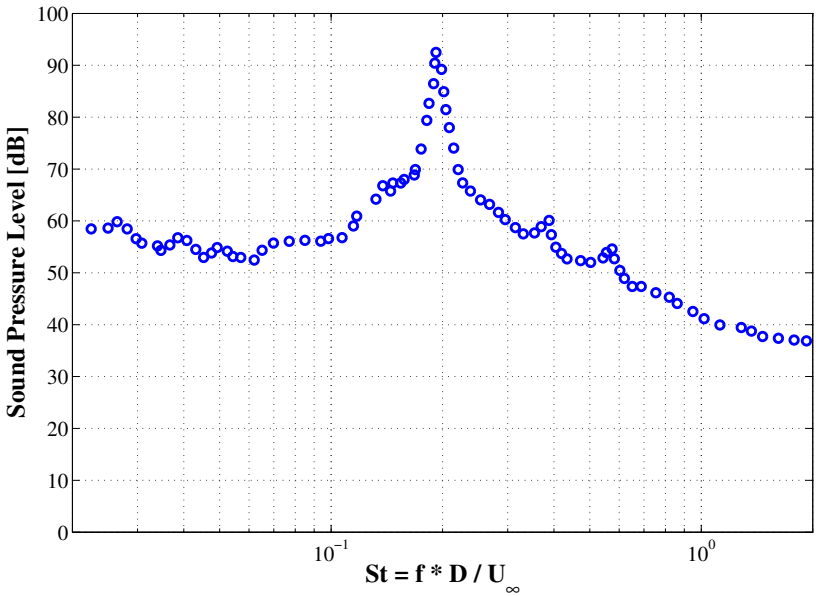

Measurement by Jacob et al.

- NACA0012 airfoil section in the turbulent wake of a circular cylinder
- Representative test case for interaction noise of various airframe components
- Good benchmark test case with tonal (cylinder shedding) and broadband (turbulent wake breakdown & impingement) components
- Farfield noise measurement made by Jacob et al.

URANS to DDES

URANS-SA

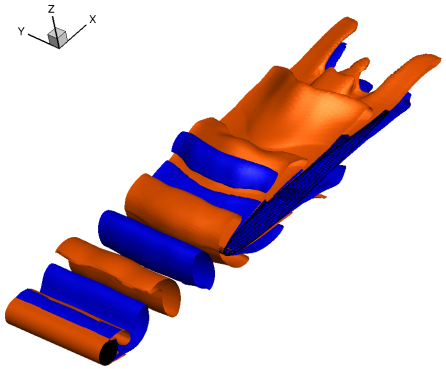

2M

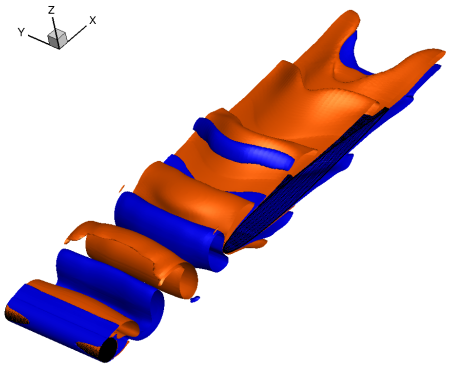

4M

DDES-SA

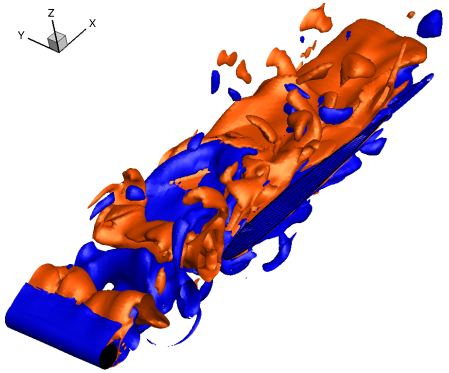

2M

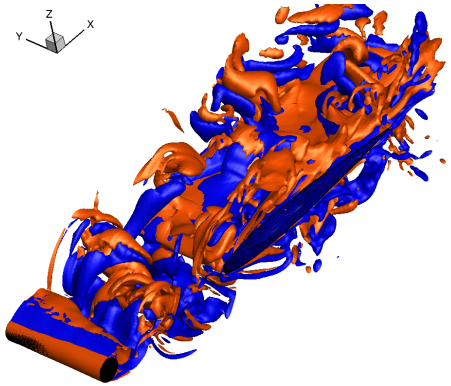

4M

- URANS+Turbulence Model: well-tuned and inexepnsive in attached boundary layer but inaccurate in separated flow
- LES cost scales strongly with Re in wall-bounded flows but accurate and independnet of Re in separated zones
- Delayed Detached Eddy Simulation (DDES): RANS in boundary layer; LES in separated region (Spalart et al., 2006)
- More refinement $\rightarrow$ more turbulent content (LES-like behaviour)
- Crucial for broadband noise prediction

Validation: 3-D Rod-Airfoil Configuration

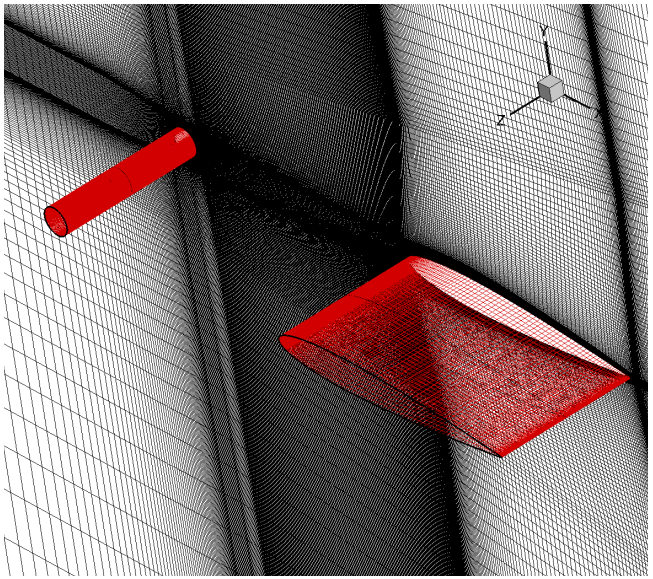

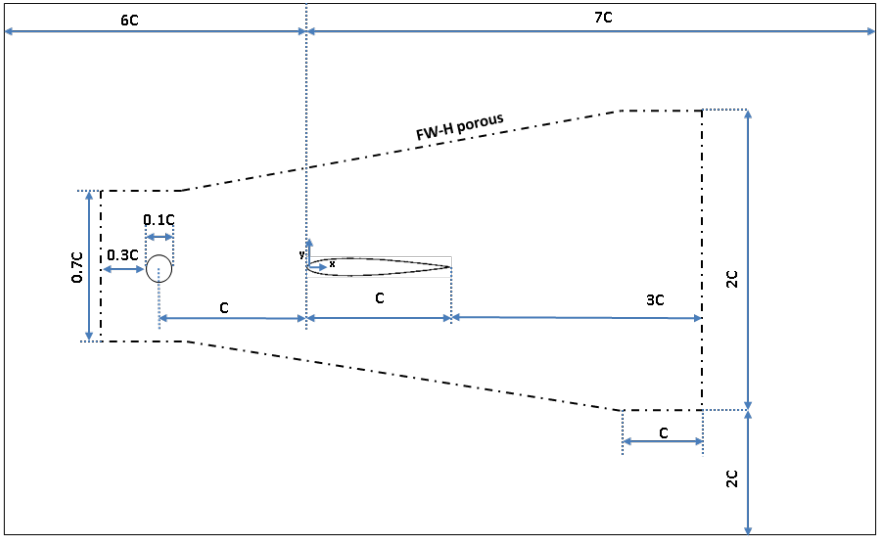

- NACA0012 airfoil section ($C = 0.1m$) with $S = 0.5C$ placed at a distance $\delta = 1.0C$ behind a cylinder of diameter $D = 0.1C$
- $U_\infty = 72m/s$, $Re_c = 4.8 \times 10^5$
- Structured mesh with ~ 6.0 million elements with refinement in rod-airfoil gap
- Nearfield acoustic source computed by DDES+SA
- Propagation to 3 farfield microphone positions ($r = 18.5C$, $\theta = 45°$, $90°$ and $135°$) using time-domain FWH.
- Farfield p' computed based on 28,500 samples, ($\sim$ 38 cycles of airfoil lift fluctuation)

Validation: Farfield Noise Spectra

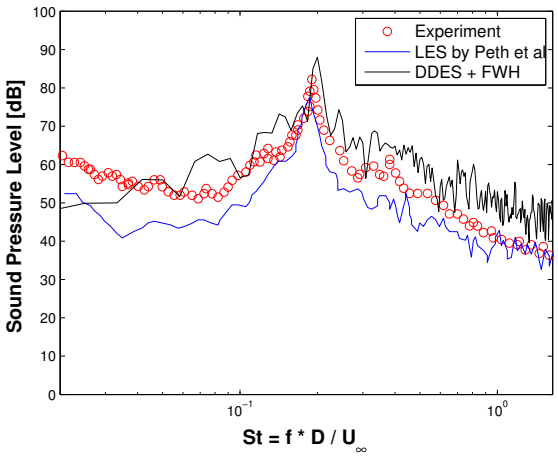

$\theta = 45^\circ$

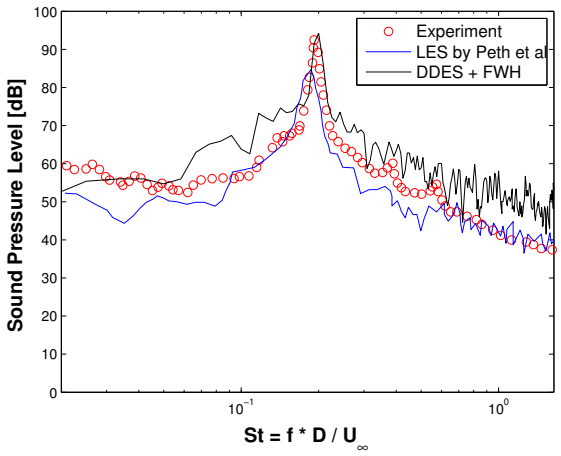

$\theta = 90^\circ$

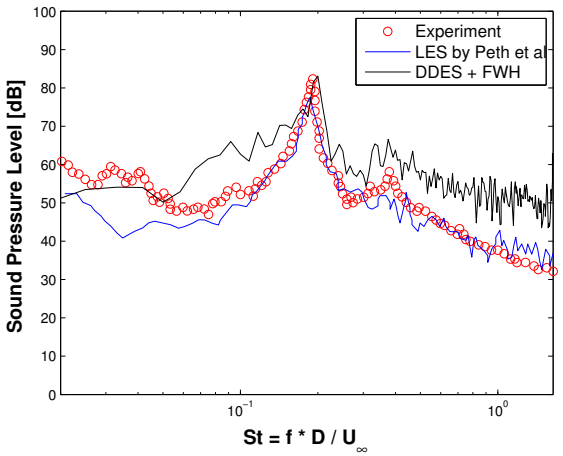

$\theta = 135^\circ$

- Good agreement with measurement around the spectral peak: tonal frequency $St = 0.19$ and peak SPL well-captured
- Low frequency error: installation effect not modeled in simulation (also noted by Giret et al. 2012)
- Broadband range over-predicted (work in progress)
  - Excessive mesh coarsening after impingement and in airfoil wake (switch back to RANS mode)
  - Spurious noise from neglecting quadrupole source (Greschner et al. 2008)

Validation: Farfield Noise Spectra

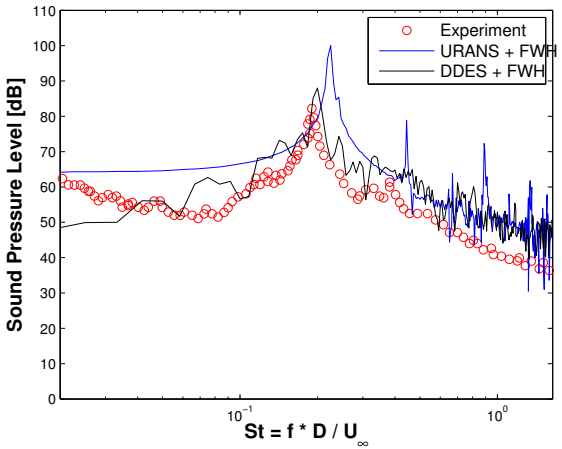

$\theta = 45^\circ$

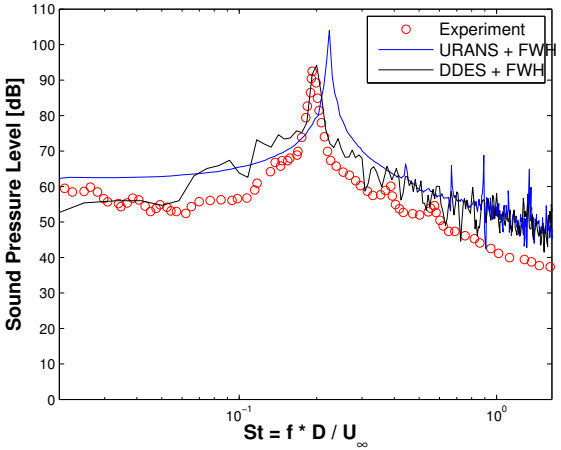

$\theta = 90^\circ$

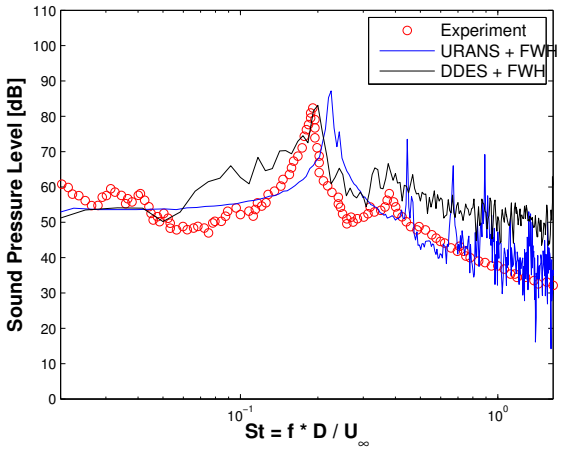

$\theta = 135^\circ$

- URANS-based results over-predict peak SPL by up to 15dB
- Tonal frequency also off by $\sim 20\%$
- Turbulent wake breakdown in rod-airfoil gap region not resolved by URANS

Noise Minimization of a Rod-Airfoil Configuration (2-D)

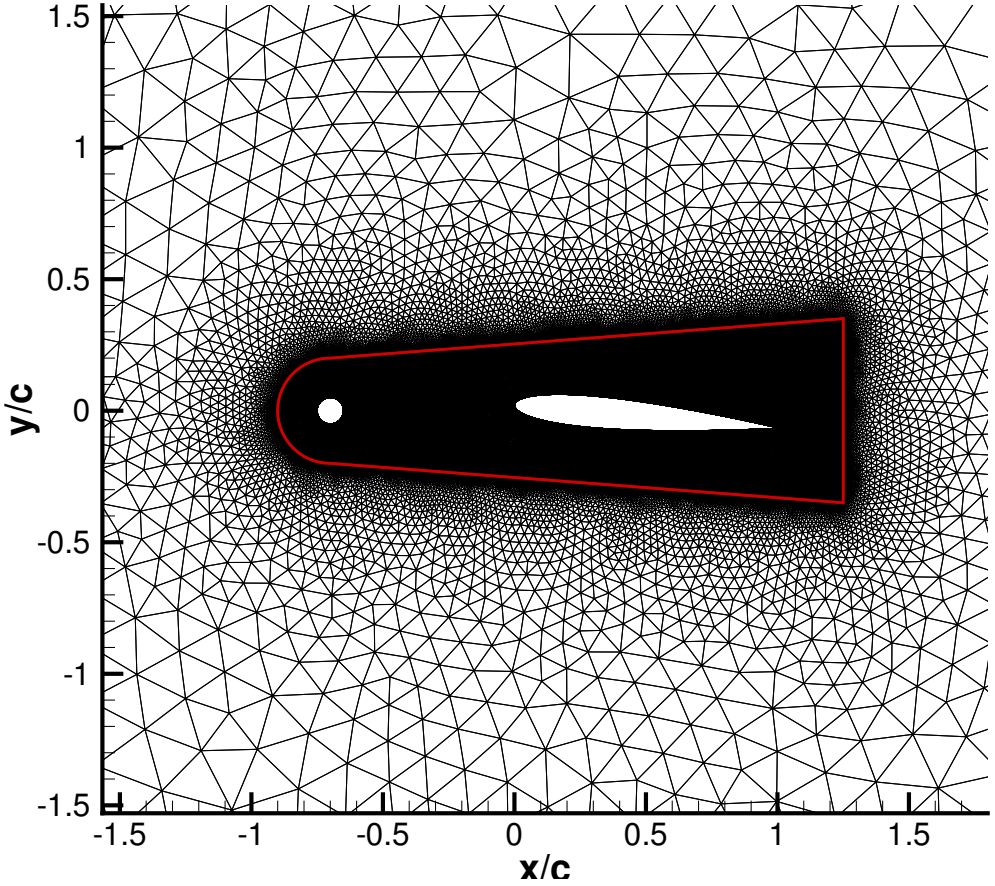

——: FWH Surface

- NACA0012 airfoil at a distance $\delta = 0.7C$ behind the cylinder
- Airfoil pitched to AoA=5°
- $U_\infty = 72m/s$, $Re_c = 4.8 \times 10^5$
- Hybrid mesh with $\sim$ 100K elements with refinement within FWH surface
- Nearfield acoustic source computed by URANS+SA
- Propagation to 3 farfield microphone positions ($r = 100C$, $\theta = 45°$, $90°$ and $135°$) using frequency-domain FWH (Lockard, 2000).
- Farfield p' corresponds to $\sim$ 9 cycles of airfoil lift fluctuation
- $J^N = RMS(p')$
- Shape design via free-form deformation(FFD) $\implies$ 256 DV's

Optimization History: Unconstrained vs. Lift-Constrained

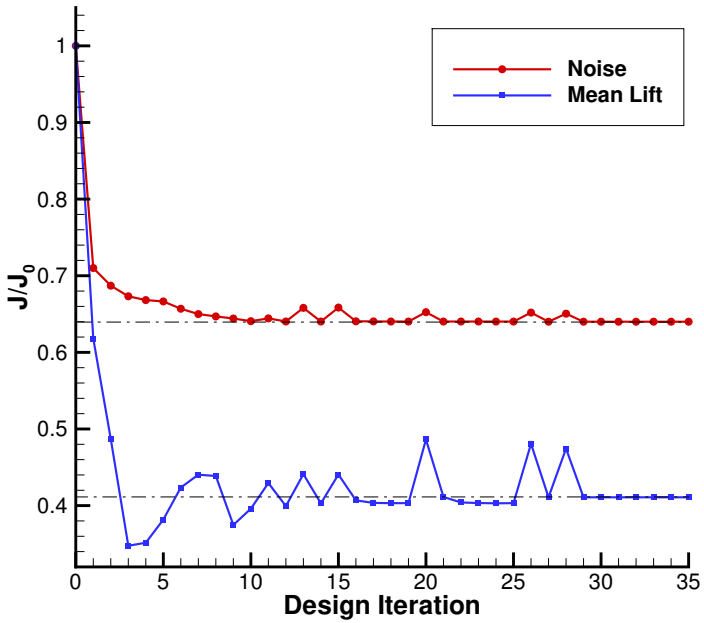

Unconstrained Noise Minimization

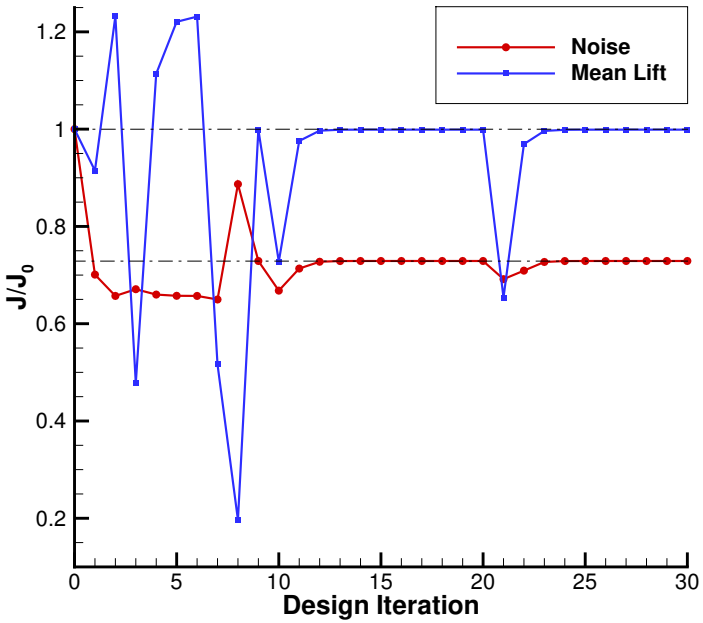

Lift-Constrained Noise Minimization

- Aeroacoustic and aerodynamic design objectives directly competing
- Unconstrained noise minimization: $\sim 36\%$ noise reduction acccompanied by marked loss of lift ($\sim 59\%$!)
- Lift-constrained noise minimization: more modest noise reduction ($\sim 27\%$) but mean lift maintained at baseline level

Acoustic Fields

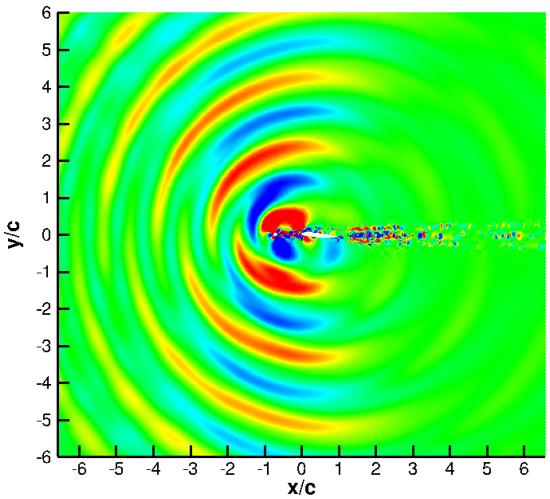

Baseline Rod-Airfoil

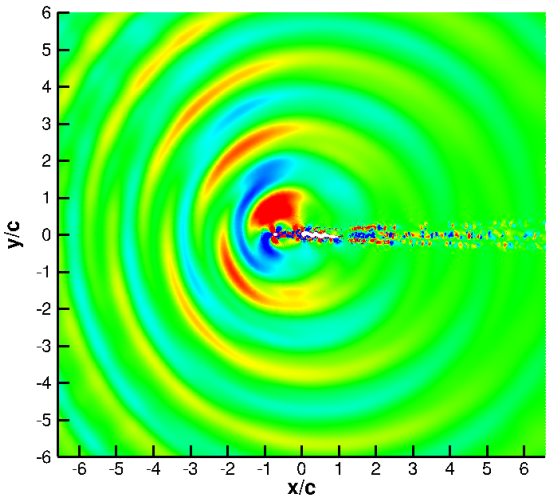

Unconstrained Noise Min.

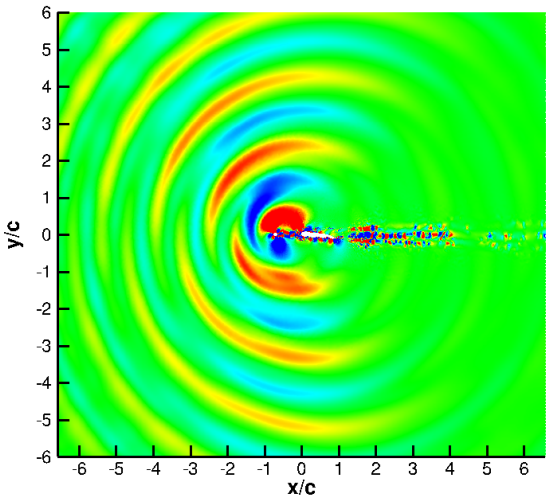

Lift-Constrained Noise Min.

- Re-computed on finer meshes for better resolution
- Dilatation field: provides a qualitative comparison of the radiated acoustic waves

Directivities and Optimized Designs

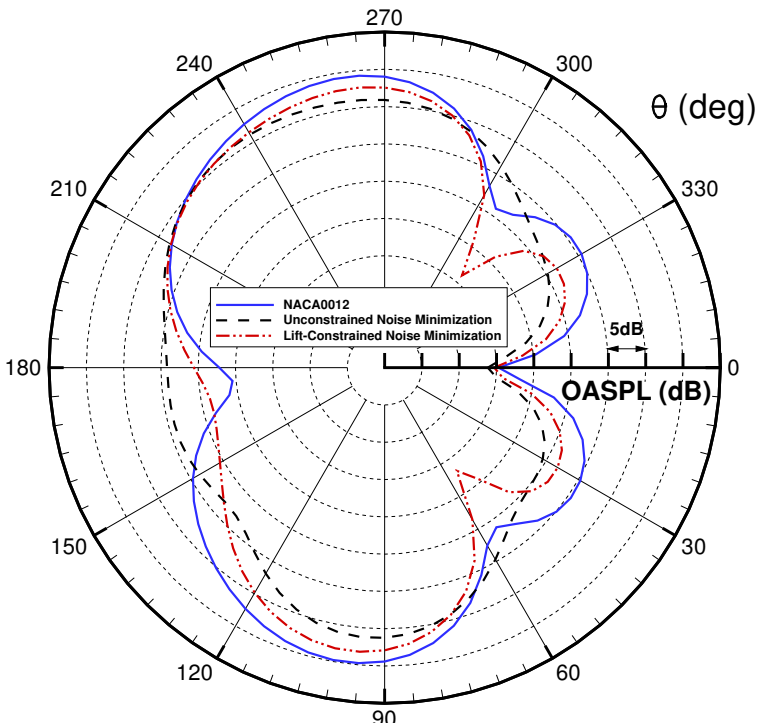

Overall Sound Pressure Level

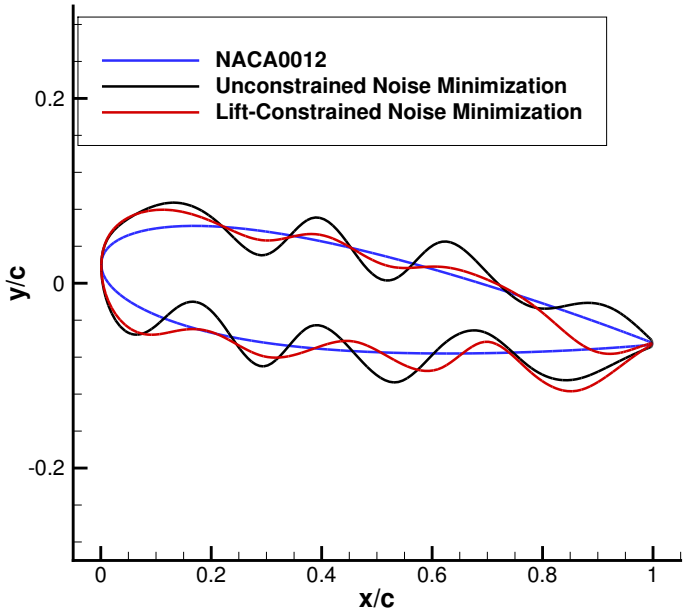

Optimized Designs

- Noise reduction in all directions with exception of shallow upstream angles
- Surface waviness in both noise-minimized and lift-constrained-noise-minimized designs
- Noted in works of other groups, mostly in spanwise waviness along LE

Noise Minimization of a Rod-Airfoil Configuration (3-D)

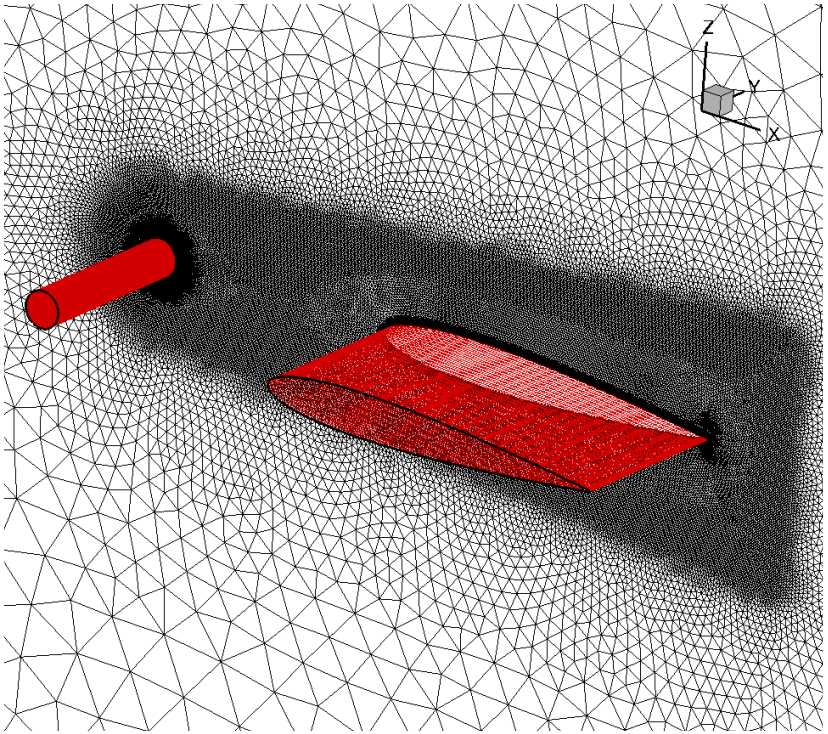

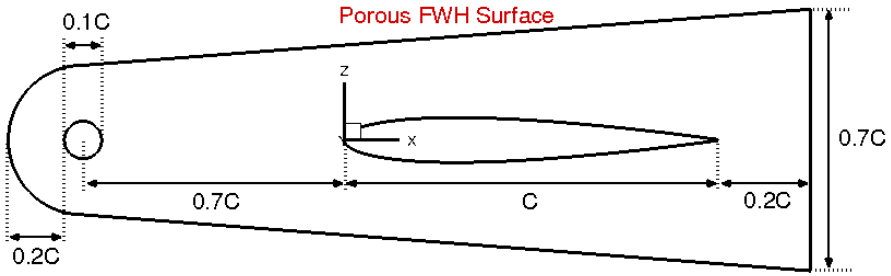

- NACA0012 airfoil section with $S = 0.5C$ placed at a distance $\delta = 0.7C$ behind the cylinder
- $U_\infty = 72m/s$, $Re_c = 4.8 \times 10^5$
- Hybrid mesh with ~ 2.8 million elements with refinement within permeable FWH surface
- Nearfield acoustic source computed by URANS+SA
- Propagation to 3 farfield microphone positions ($r = 100C$, $\theta = 45^\circ$, 90° and 135°) using time-domain FWH.
- Farfield p' corresponds to ~ 10 cycles of airfoil lift fluctuation

Optimization History

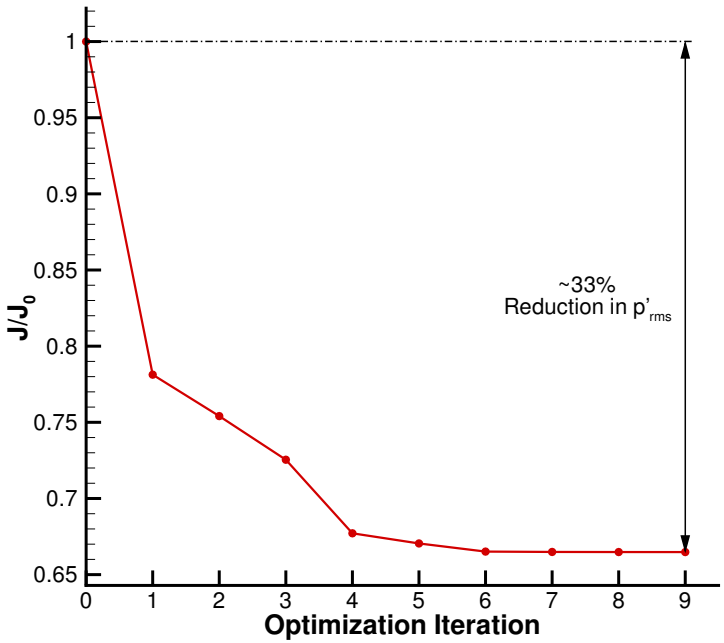

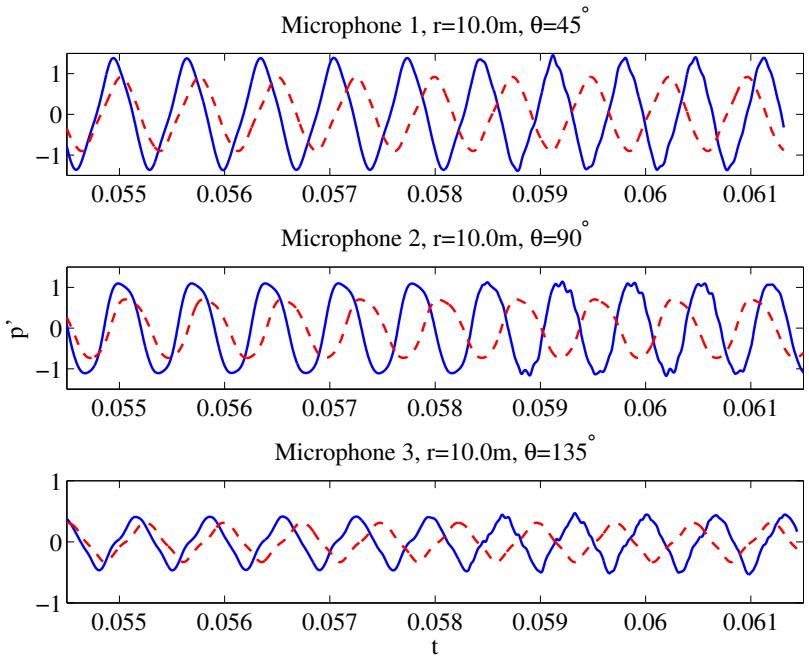

——: Baseline; – – –: Optimized

- 33% reduction in $J^N = \sqrt{\overline{(p')^2}}$ after 9 design iterations
- No aerodynamic or geometric design constraints applied
- Clear farfield noise reduction in all three directions ($\theta = 45^\circ$, 90° and 135°)

Optimization History

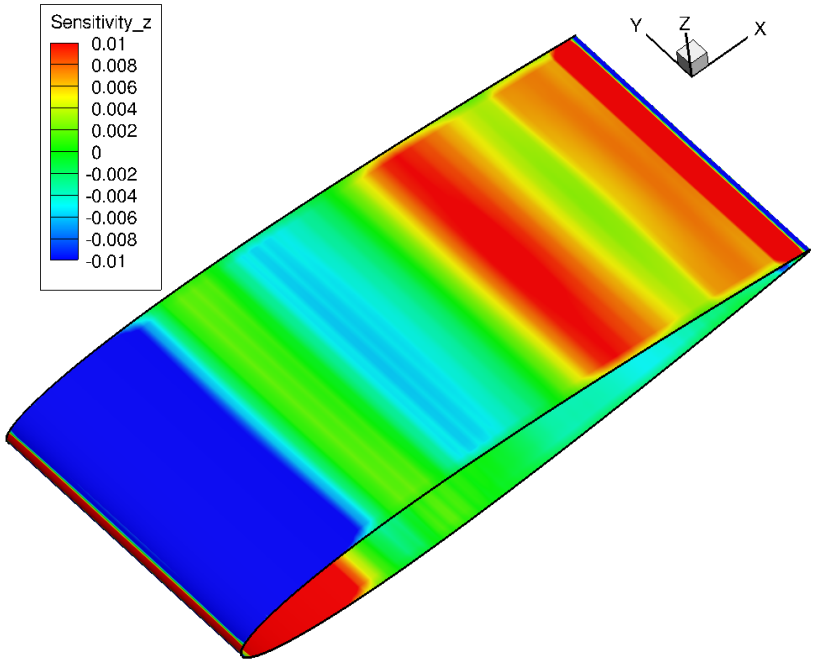

Surface noise sensitivity in normal direction

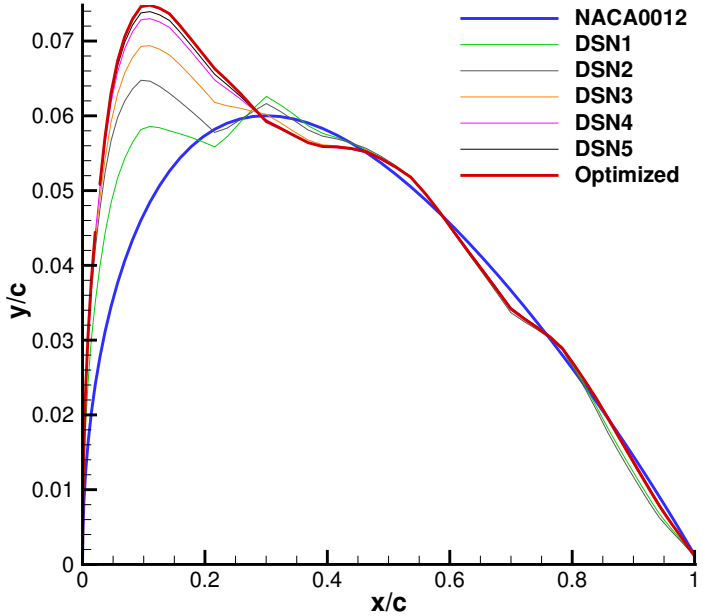

Design Evolution

- Does not collapse the airfoil as one would expect
- Optimizer introduces streamwise waviness on both upper and lower surfaces
- No spanwise variation in surface sensitivities – due to coherent vortices impinging on the airfoil LE due to URANS simulation
- Scale-resolving simulations required to model turbulent wake breakdown

DDES Simulation of Nearfield Acoustic Sources

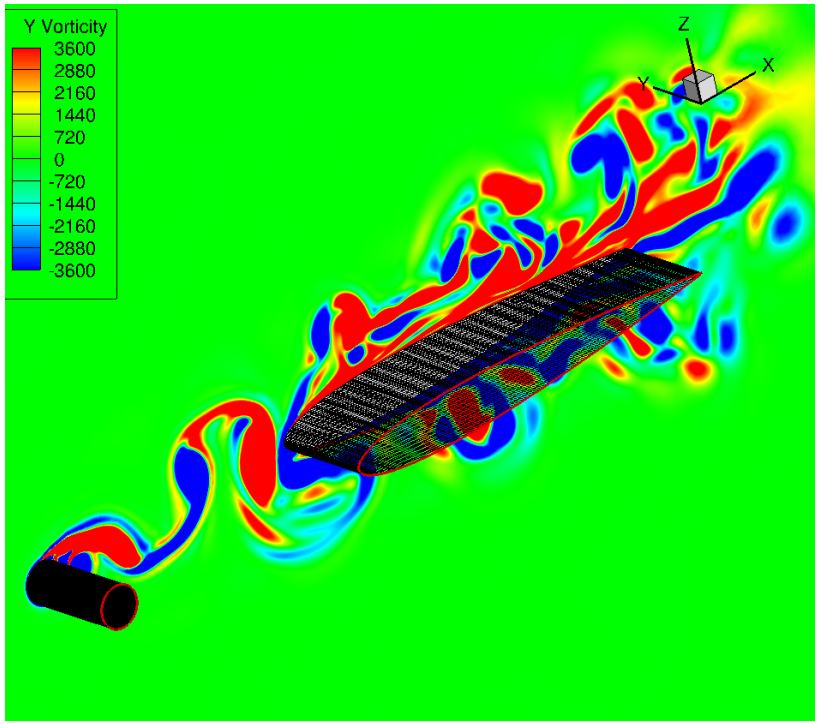

Baseline

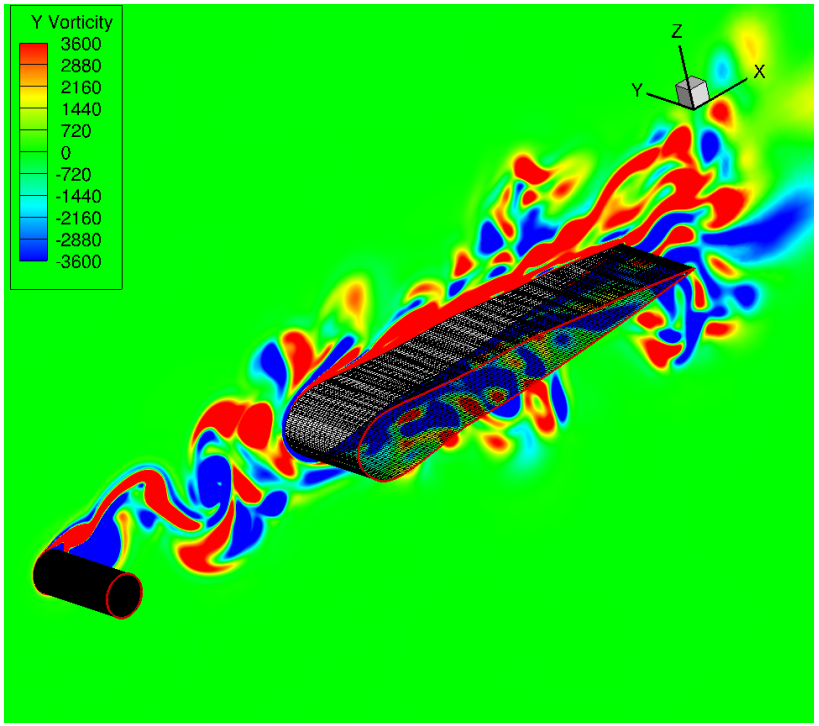

Optimized

- Hybrid mesh with 4 million elements with extra refinement in cylinder wake region to encourage RANS-LES switch
- Surface waviness ‘surpresses’ noise-generating vortical structures from the airfoil surface

Acoustic Results Based on DDES-FWH

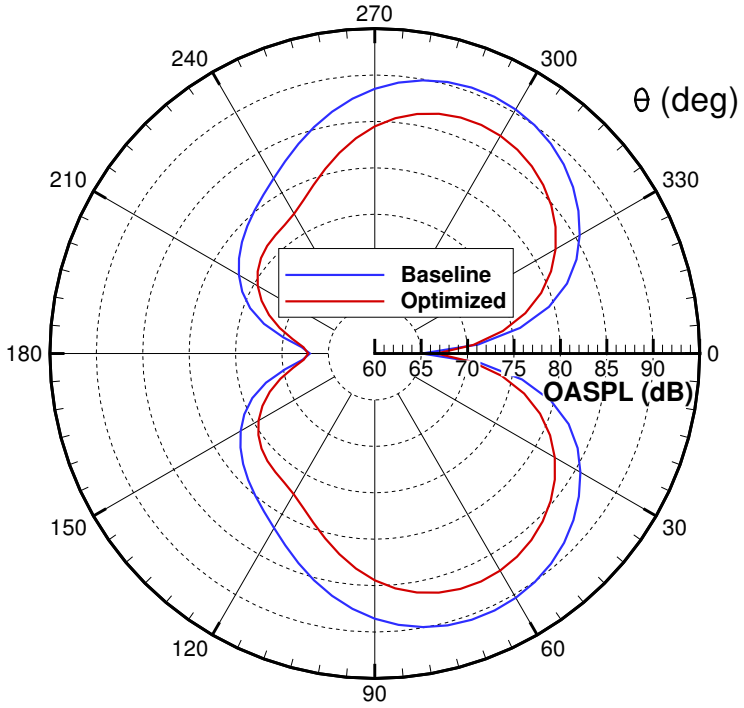

Overall Sound Pressure Level

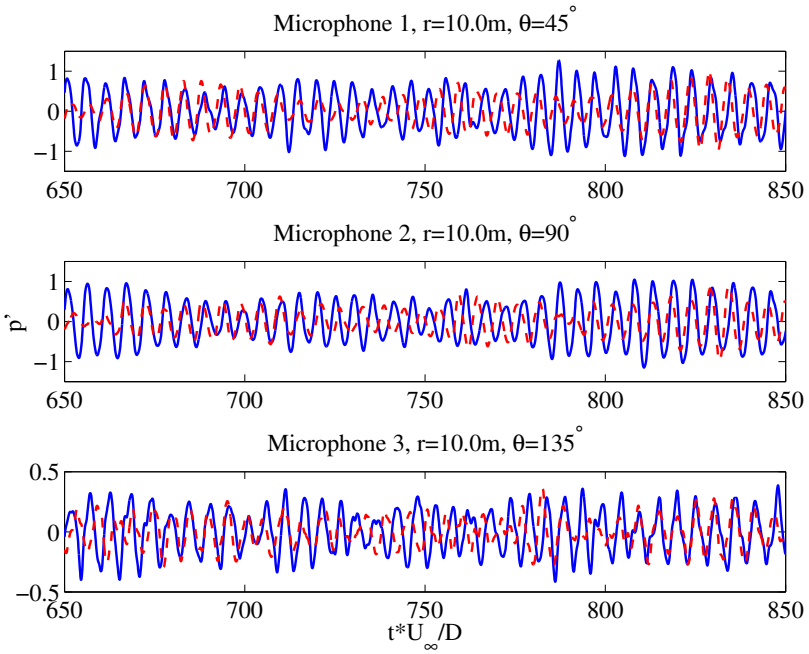

——: Baseline; – – –: Optimized

- Sample collection after 50 flow passage times
- 15000 samples corresponding to $\sim$ 40 cycles of lift fluctuations on airfoil
- J^N reduced by $\sim$ 45% (compared to 33% with URANS-FWH)
- OASPL: omni-directional noise reduction, up to 6dB

Farfield Noise Spectra (R = 100C)

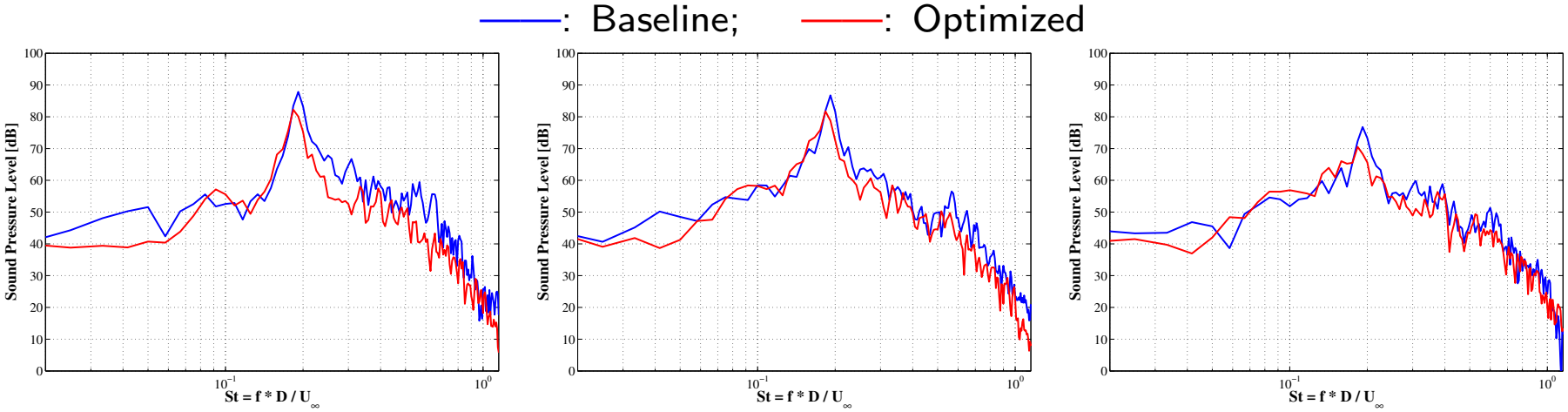

$\theta = 45^\circ$ $\theta = 90^\circ$ $\theta = 135^\circ$

- Peak frequency $St = 0.19$ well-captured in baseline configuration
- Peak SPL reduced by 5-6 dB
- Broadband reduction not omni-directional, but at least peak SPL not shifted towards higher frequency
- To minimize broadband noise, J^N must be re-defined to target high-frequency component $\implies$ perform optimizations directly with DDES-FWH in the loop

LE and TE Modifications

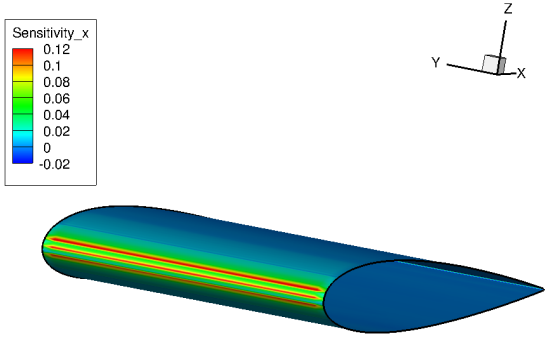

- LE and TE serration/waviness already shown to have acoustic and aerodynamic benefits

Adjoint Optimization

with DDES+FWH?

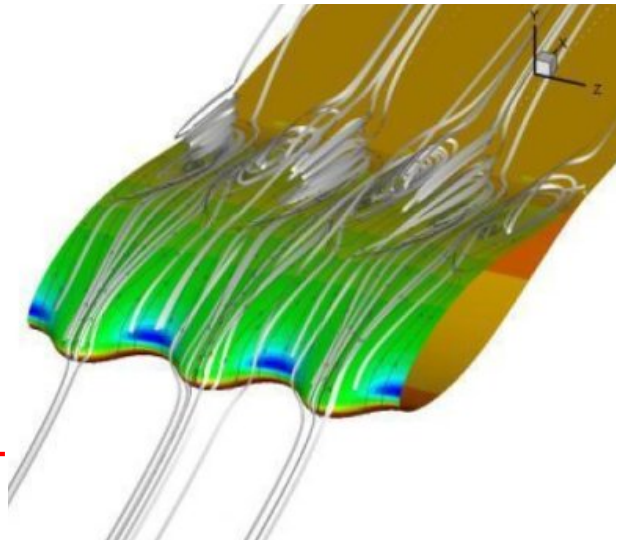

Credit: Fish et al. Integrative and Comparative Biology, 2008

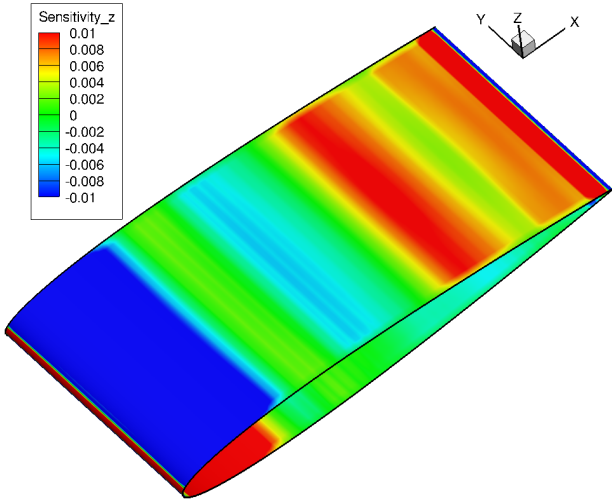

- Can they be further optimized?
- More importantly, can noise reduction be achieved with aerodynamic design constraints at practical flow regimes ($Re \sim 10^7$)?

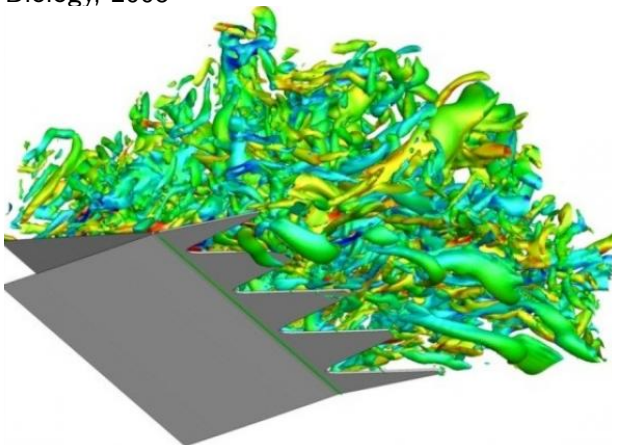

Credit: L. Jones and R. D. Sandberg, Journal of Fluid Mechanics, 2012

Summary and Future Work

Summary

- 2D & 3D FW-H acoustic solver implemented in SU2, coupled with URANS and DDES
- Adjoint-based aeroacoustic design enabled by a discrete adjoint solver based on algorithmic differentiation (AD)
- Aeroacoustic and aerodynamic design objectives shown to be competing
- Streamwise surface waviness observed in optimized airfoil with 5-6 dB noise reduction (scale-resolving methods required to exploit spanwise variations)
- Validation against experiment: tone well-captured; broadband to be improved

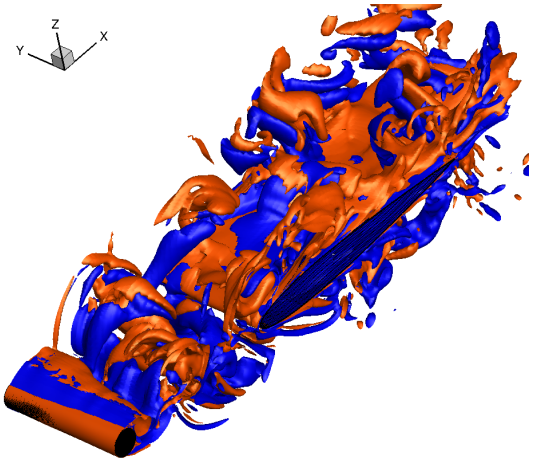

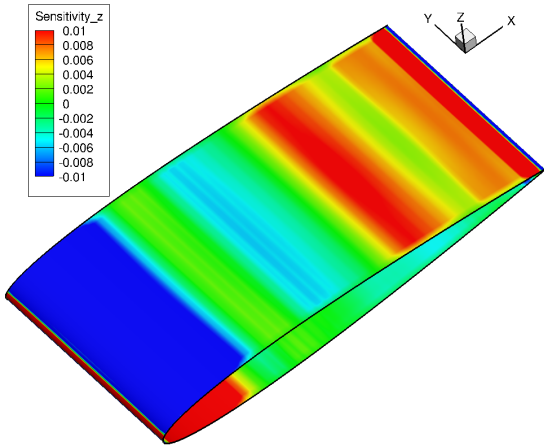

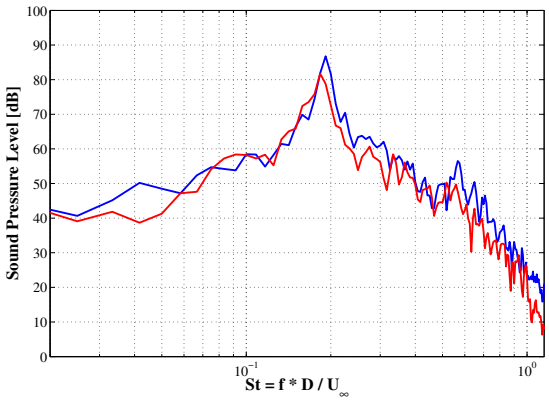

Summary and Future Work

Future Work

- Further validate the DDES-FWH solver in SU2 against various benchmark cases

Summary and Future Work

Future Work

- Further validate the DDES-FWH solver in SU2 against various benchmark cases
- Adjoint-based noise minimization to tackle broadband noise – much more challenging to remove/reduce than tonal noise
  - Challenge #1: Mesh size for DDES $\sim O(10^{7-8})$ for large, complex geometries
  - Challenge #2: Need for regularization due to chaotic LES content

Summary and Future Work

Future Work

- Further validate the DDES-FWH solver in SU2 against various benchmark cases
- Adjoint-based noise minimization to tackle broadband noise – much more challenging to remove/reduce than tonal noise
  - Challenge #1: Mesh size for DDES $\sim O(10^{7-8})$ for large, complex geometries
  - Challenge #2: Need for regularization due to chaotic LES content
- Synthetic-turbulence-type methods (e.g. SNGR) for noise generation based on (U)RANS solutions at lower cost
  - Joint work with Lars Davidson's group at Chalmers University to commence in April 2018

Summary and Future Work

Future Work

- Further validate the DDES-FWH solver in SU2 against various benchmark cases
- Adjoint-based noise minimization to tackle broadband noise – much more challenging to remove/reduce than tonal noise
  - Challenge #1: Mesh size for DDES $\sim O(10^{7-8})$ for large, complex geometries
  - Challenge #2: Need for regularization due to chaotic LES content
- Synthetic-turbulence-type methods (e.g. SNGR) for noise generation based on (U)RANS solutions at lower cost
  - Joint work with Lars Davidson's group at Chalmers University to commence in April 2018
- Can URANS-SNGR-FWH provide 'accurate enough' characterization of farfield noise (compared to DDES-FWH) for optimization?

Summary and Future Work

Future Work

- Further validate the DDES-FWH solver in SU2 against various benchmark cases
- Adjoint-based noise minimization to tackle broadband noise – much more challenging to remove/reduce than tonal noise
  - Challenge #1: Mesh size for DDES $\sim O(10^{7-8})$ for large, complex geometries
  - Challenge #2: Need for regularization due to chaotic LES content
- Synthetic-turbulence-type methods (e.g. SNGR) for noise generation based on (U)RANS solutions at lower cost
  - Joint work with Lars Davidson's group at Chalmers University to commence in April 2018
- Can URANS-SNGR-FWH provide 'accurate enough' characterization of farfield noise (compared to DDES-FWH) for optimization?
- SU2-ANOPP2 coupling for propeller design (joint work with Len Lopes, NASA Langley)

Summary and Future Work

Future Work

- Further validate the DDES-FWH solver in SU2 against various benchmark cases
- Adjoint-based noise minimization to tackle broadband noise – much more challenging to remove/reduce than tonal noise
  - Challenge #1: Mesh size for DDES $\sim O(10^{7-8})$ for large, complex geometries
  - Challenge #2: Need for regularization due to chaotic LES content
- Synthetic-turbulence-type methods (e.g. SNGR) for noise generation based on (U)RANS solutions at lower cost
  - Joint work with Lars Davidson's group at Chalmers University to commence in April 2018
- Can URANS-SNGR-FWH provide 'accurate enough' characterization of farfield noise (compared to DDES-FWH) for optimization?
- SU2-ANOPP2 coupling for propeller design (joint work with Len Lopes, NASA Langley)
- System-level optimization with OpenMDAO (joint work with Justin Gray, NASA Glenn)

Acknowledgements

- Computing resources provided by the "Alliance of High Performance Computing Rheinland-Pfalz" (AHRP), via the "Elwetritsch" Cluster at the TU Kaiserslautern
- Financial support from the Canadian Postgraduate Scholarship (NSERC-PGS-D)

Thank you for your attention